Calcif Tissue Int (1984) 36:550–555

Calcified Tissue International

Length and Shape of Enamel Crystals

G. Daculsi, J. Menanteau, L. M. Kerebel, and D. Mitre

U 225 INSERM, Faculté de Chirurgie Dentaire, Place A. Ricordeau, 44 042 Nantes, France

Summary. An original method for fractionating and preparing isolated crystals of homogeneous size was developed. It was demonstrated that enamel apatite crystals are at least 100 μm long. The flexibility of the very long crystallites was demonstrated. Crystal curvatures, accounting for the irregular course of the prisms through the enamel thickness, were visualized and measured. It was shown that in the deep forming enamel layer, lateral branches may grow out of the crystals and crystal fusing often occurs, inducing the crystallites to assume pyramidal shapes with their wide bases pointing toward the dentino-enamel junction and one or two tops toward Tomes' processes. During the maturation process, the two tops of the still immature crystals also fuse so that the mature crystals acquire a rodlike aspect, with parallel faces and steplike graduations along the *c* axis, allowing a close contact between the crystals. These results support the hypothesis that the crystallites would be continuous from the dentino-enamel junction to the surface.

Key words: Enamel crystals — Length — Shape — Apatite — Ultrastructure.

The morphology and size of enamel crystals could not be determined precisely until high resolution TEM techniques were available. Previously published measurements were the result of classical TEM or X-ray diffraction studies [1–8]. Ultramicrotomy was proved to produce artifacts when applied to calcified tissues [9, 10] and consequently did not allow for measuring crystal length. Whatever the technique might be—X-ray diffraction or SEM [11]—length measurements were approximate. Present-day high resolution methods allow identification of the section plane, performed on ultrathin sections, and hence provide accurate measurements of both crystal width and thickness [12–14]. However, they do not permit determination of crystal length and shape related to the *c* axis.

In the present investigation, a new method for fractionating calcifying tissues according to density variations was used to study the shape and size of the crystals during the developing process.

Send reprint requests to G. Daculsi at the above address.

Materials and Methods

Embryonic enamel pieces were obtained from tooth germs of human fetuses and newborn pigs and veals, fixed with 2% glutaraldehyde and postfixed with 1% osmium tetroxide solution in cacodylate buffer pH 7.4. The undecalcified specimens were dehydrated in a graded series of methanol concentrations, embedded in methacrylate, and ultrathin sections were performed with a Sorvall Porter ultramicrotome equipped with diamond knives to be examined with a JEOL 100 B TEM operating at 100 kV.

Other germs were immediately frozen upon removal. The soft immature enamel layer at the dentinal surface was gently scraped off and powdered under liquid nitrogen in a Spex Mill, five times during 1 min. The proceedings of the new density fractionation method used in the present investigation have been thoroughly described and discussed in another paper (Menanteau et al. [24]) and will be briefly summarized here.

The enamel powders were separated into different fractions corresponding to different densities, using cesium chloride refrigerated solutions whose densities ranged between 1.9 and 1.6 at 25°C. The collected fractions were dialyzed for 4 days against 4 M guanidinium hydrochloride pH 8.8. This method removes the greatest part of the organic material which, at this stage of development, mainly consists of amelogenins.

The residues were thoroughly rinsed with deionized water. The crystals were laid down under water on a Cu grid covered with carbon-coated formvar and examined with a JEOL 100 B TEM operating at 100 kV.

Crystal curvatures were calculated using the Frenet's mathematical method which defines the curvature on a point of a planar curve f (t) with x (t) and y (t) parameters:

$$p(t) = \frac{|x'y'' - x''y'|}{[(x')2 + (y')2]3/2}$$

x′ and y′ = first derivative
x″ and y″ = second derivative

Results

Ultrathin Sections

Examination of cross-sections of embryonic dental enamel prisms showed them to assume the classical keyhole aspect (Fig. 1). Electrolucent spaces between adjacent prisms were filled with methacrylate, which indicates that they were not due to artifacts of preparation and sample handling. Examination of earlier stages of enamel formation at higher magnifications showed the junction between two prisms to consist of a space 1,000–2,000 nm wide, free from crystallites (Fig. 2). At this stage, the crystals appeared as long, thin, and flexuous ribbons located within the heads of the prisms, the sectioned crystals of two adjacent prisms forming an acute angle with each other. In the tails of the prisms sectioned perpendicular to their long axis, the crystallites were distributed according to this long axis (Fig. 3). Consequently, these crystallites were sectioned perpendicular to their *c* axis, with haphazard orientation of the *a* and *b* axes, the crystals being then distributed without any preferred orientation with respect to each other. *Some of them assumed a Y shape when viewed in cross-section (Fig. 3). High resolution TEM examination demonstrated that this aspect could not be due to overlapping of the crystals but was actually related to crystal branches induced by fusions or lateral growing.*

Isolated Crystals

Observations focused on crystals obtained from homogeneous fractions whose densities ranged between 1.8 and 1.6. They showed rodlike crystallites, all very long, the longest ones even projecting beyond the visual field bounded by the edges of the copper grids, that is, 100 μm (Fig. 4). These crystals, 40–50 μm long, were laid flat on the formvar film according to their long axis. It was then possible to measure their minimal length and to form a correct estimate of their shape with respect to the c axis.

Electron diffraction of isolated single crystals (Fig. 5) corroborated the TEM data, showing the crystals to belong to the apatitic hexagonal system.

Considerable variations were recorded in crystal width all along the *c* axis. These variations involved both narrowing and enlarging due to an increase in the *a* and *b* parameters which induced projections and steps occurring all along the cystals (Figs. 6, 7). Also, the long crystals observed were sinuous and flexible enough to allow marked curvatures. (Figs 8, 9).

Another feature was the forking of some crystals into parallel branches. Figure 8 shows a single length of crystal bifurcating twice into three parallel segments. Sometimes it seemed that one of the branches broke and flipped 180° about its *c* axis (Fig. 10).

Crystal curvatures always occurred according to the narrowest part of the crystal, (thickness), just like a ribbon. The crystallites layed flat on the formvar film bended and were viewed in profile, then bended again to lay flat on the film (Fig. 11). However, the flexibility of the crystals was limited; it was observed that strongly marked flexions induced fractures at the bending level (Fig. 12). The smallest value obtained for crystal curvature was 0.1 μm.

Discussion

High resolution TEM allows for determination of the section plane of a crystal and provides accurate measurements of both width and thickness of human enamel crystals to within a few Angströms (263 Å ± 22 × 683 Å ± 34). However, the method does not permit accurate length determination. Rönholm's evaluation [5] of the length of human enamel crystals is 1,600 Å, Nylen et al.'s [15], and Selvig and Halse's estimate [16] is 1,500 Å, a value which, according to them, would remain unchanged during the maturation process. In our opinion, the only available method for obtaining accurate length measurements is to prepare isolated crystallites.

The technique described here is based on the solubilization of the main part of the organic matrix of powdered immature enamel samples from which a suspension of separate crystals is obtained. Despite the fact that the grinding process induces a breaking of the longest crystals, we obtained length values beyond 100 μm. Considering the limits of the observed field during TEM procedures, it is most likely that the real size of these crystals is much larger, which corroborates the hypothesis developed by Warshawsky and Nancy [17] on the basis of a stereological study. Length must be considered as infinite with respect to section thickness. Thus, even if crystallites have true "ends," these would probably never be recognized in TEM sections. It

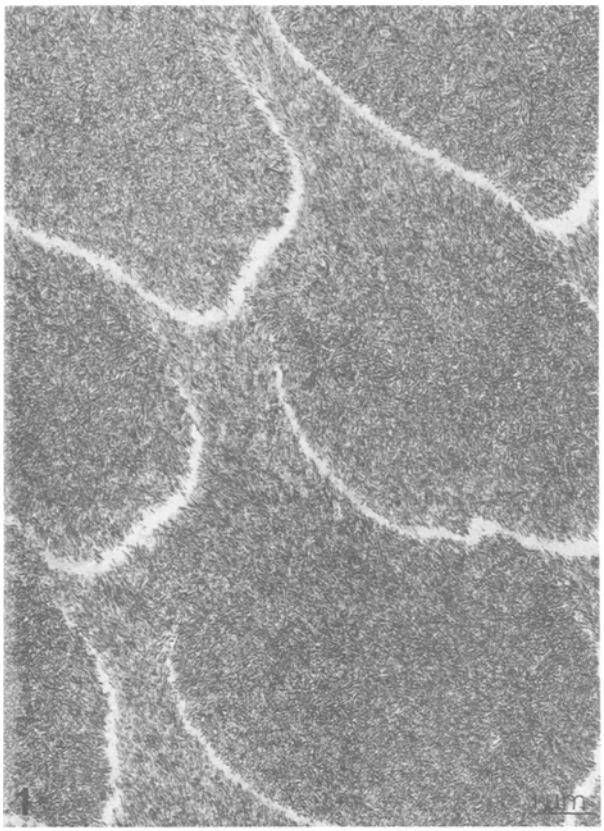
1
0,1µm

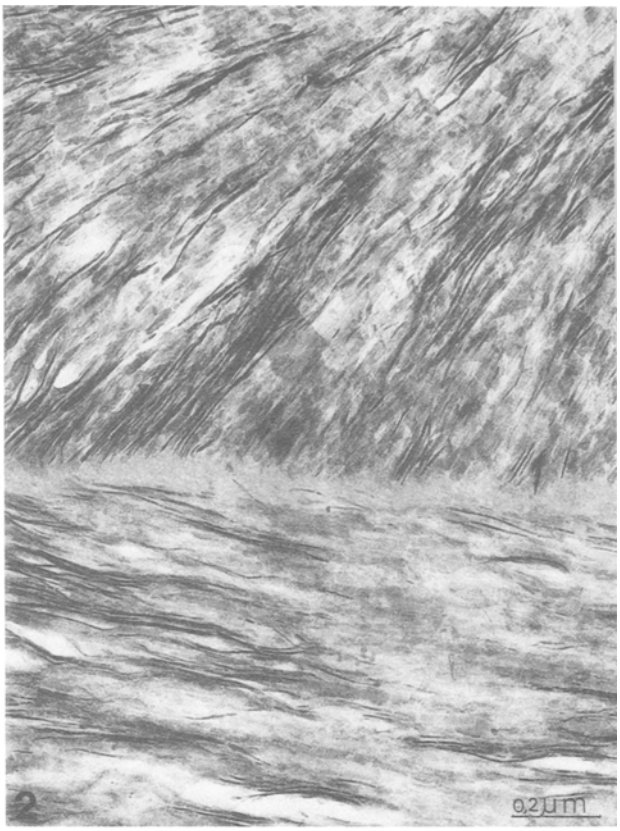
2
0,2µm

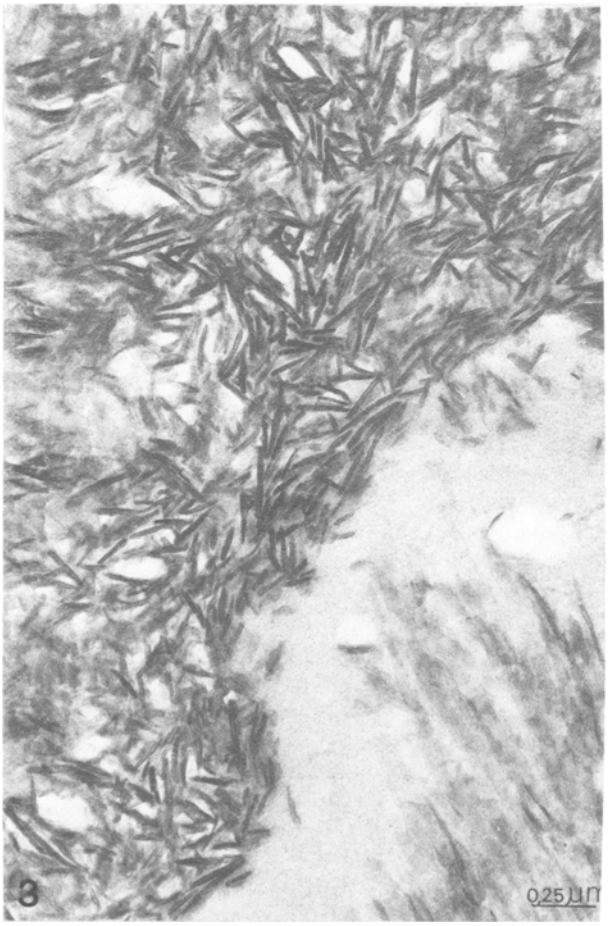
3
0,25µm

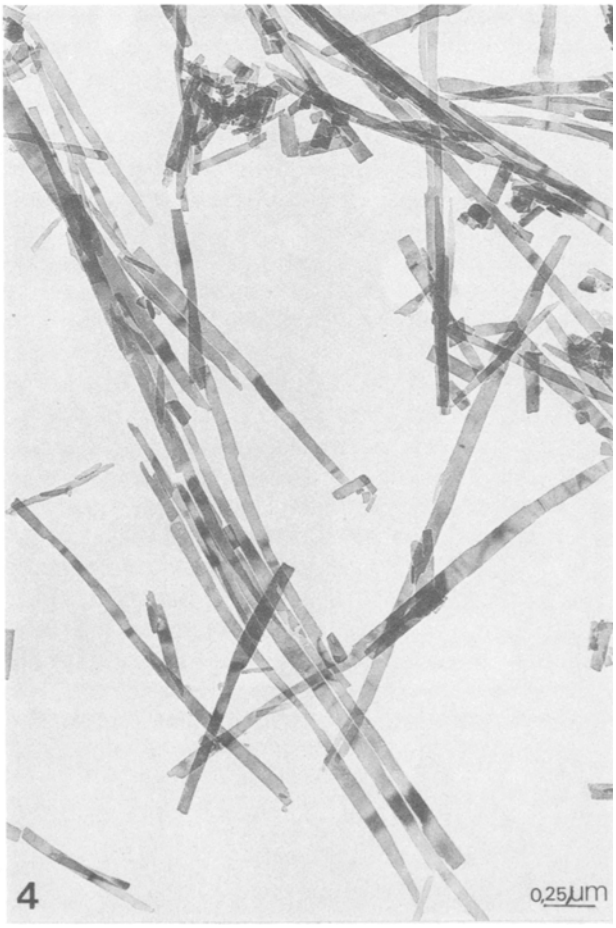
4
0,25µm

Fig. 1. Cross-section of embryonic enamel prisms. TEM × 10,000.

Fig. 2. Aspect of the junction between two enamel prisms. TEM × 38,000.

Fig. 3. Crystal distribution within the tails of the prisms. Also note the Y shape assumed by some crystallites. TEM × 67,000.

Fig. 4. Length of the isolated crystals. TEM × 31,000.

seems that enamel crystals extend without interruption from their beginning at the dentino-enamel junction to their ends at the enamel surface.

However, if the apatite crystals are continuous from the dentino-enamel junction to Tomes' processes, two comments must be made, the first one being closely related to the morphology of the enamel prisms. Helmcke [18] as well as Leblond and Warshawsky [19] unambiguously demonstrated the irregular course of the prisms through the enamel thickness. Consequently, the individual crystals within the prisms will not be straight either. Long flexuous crystal ribbons are classically described within the early mineral deposits during enamel formation. Crystal defects (dislocations) inducing crystal curvatures have been previously visualized with high resolution TEM [13, 14]. The incidence of these defects upon the curvature radius has been calculated [20]. The results of the present investigation clearly demonstrate the existence of these curvatures even when local stresses related to the morphology of the prisms and the relative flexibility of biological apatites cannot be involved. It is most likely that the smallest value (0.1 μm) obtained for crystal curvature represents the maximal strain that can be supported by the crystal before splitting occurs, as it was visualized in the present investigation. However, it is not possible to ascertain whether the curvatures observed on isolated crystals are artifacts or not.

The second point relates to the increase in the mineralization degree. In our opinion, and in disagreement with Hammarlung-Essler's assessment [21], the increasing degree in enamel mineralization is not due to an increase in the number but rather in the size of the crystallites. According to Ronholm [5], the progressive increase in enamel mineralization is related to an increase in both thickness and width of enamel crystallites. In a previous study concerning embryonic human enamel [13], this increasing process was shown to be a logarithmic increase in width with respect to thickness. Since the enamel volume does not increase when the crystals get thicker in the course of mineralization, two possibilities may be considered: the first is that a certain number of crystallites actually disappear or fuse together in the course of the maturation process. In the above-mentioned study [13], the crystallites were numbered per volume unit and a loss of half of the crystallites was found in mature enamel compared with the first layers of enamel mineralization. If the crystallites are continuous from the dentino-enamel junction to the surface, it means obviously that the earliest crystallites, located near Tomes' processes, join in the course of the thickening process and finally fuse, which explains the variations in the number of crystallites through the different stages of mineralization. The fusing first occurs in depth, whereas the crystallites remain narrow and separated from each other at the surface. At their mature stage, the crystallites are no longer pyramidal but assume a regular rodlike aspect. As a result of fusing associated with growing in width and thickness, the crystallites fill all free spaces left between each other and acquire a classical rodlike shape, with steplike graduation along their length. Similar irregular shapes have been described in studies performed on isolated crystals [22].

The second possibility involves an ancillary growth of the crystals. It can be seen from Figure 8 that the total width of the three parallel segments observed is approximately three times that of the unsplit segment. Thus, it is most likely that the parallel or split segments are "daughter crystals" branching from a single parent.

Both explanations may be retained. Fusions and ancillary growth phenomenons have been demonstrated using high resolution TEM. For instance, it has been demonstrated that the fusions of adjacent crystals result in irregular shapes and disregistry of the lattices (grain boundaries, linear dislocations) [13].

In conclusion, our results fit well with Meckel et al.'s "classical" model [23], which is related to the distribution of the crystallites within the prisms. They fit well also with the studies dealing with the shapes of the crystallites [18]. Our results demonstrate the large length of enamel crystallites, their pyramidal shapes, and their steplike morphology all along the *c* axis. They clearly show the extent to which the crystallites can flex without breaking and the bifurcations occurring along the crystal length. However, other studies should be conducted before

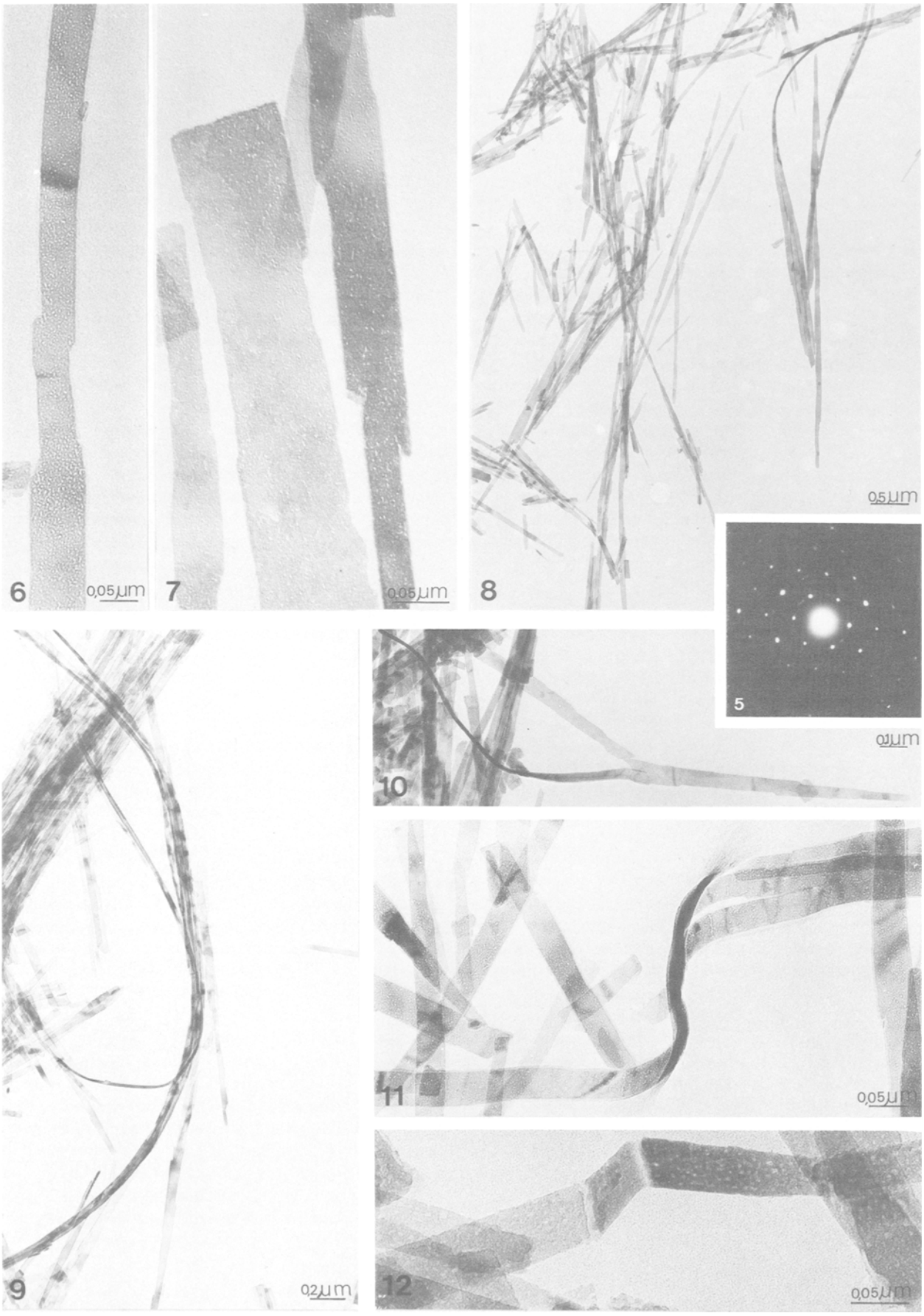
6
0,05 µm
7
0,05 µm
8
0,5 µm
5
0,1 µm
10
9
0,2 µm
11
0,05 µm
12
0,05 µm

Fig. 5. Electron diffraction of the isolated crystals.

Fig. 6. Variations in crystal width along the *c* axis. TEM × 150,000.

Fig. 7. Projections and steps occurring all along the crystal length. TEM × 225,000.

Fig. 8. Sinuous aspect of the long crystals. Note how a single length of crystal bifurcates twice into three parallel segments. TEM × 15,000.

Fig. 9. Sinuous aspect of the long crystals. TEM × 35,000.

Fig. 10. Two daughter crystals branching from a single parent. One of the branches has broken and flipped 180° about its *c* axis. TEM × 52,000.

Fig. 11. Different aspects of crystal curvatures. TEM × 150,000.

Fig. 12. Strong flexions inducing fractures at the bending level. TEM × 235,000.

definitely concluding that the crystallites are continuous from the dentino-enamel junction to the enamel surface. These studies should involve crystal distribution within the prisms and between the prisms.

Acknowledgments. The authors wish to thank Isabelle Jans for her technical assistance.

References

1. Jensen AT, Möller A (1948) Determination of size and shape of the apatite particules in different dental enamels and in dentine by the X-ray powder method. J Dent Res 27:524
2. Little K (1955) Electron microscope studies of teeth. J Dent Res 34:778
3. Little K (1959) Electron microscope studies on human dental enamel. J R Micr Soc 78:58–66
4. Frank RM, Sognnaes RF, Kern R (1960) Calcification of dental tissues with special reference to enamel ultrastructure. In: Sognnaes RS (ed) Calcification in biological systems. American Association for the Advancement of Science, Washington DC, pp 163–202
5. Rönnholm E (1962) The amelogenesis of human teeth as revealed by electron microscopy. II: the development of the enamel crystallites. J Ultrastruct Res 6:249–303
6. Nylen MU (1964) Electron microscope and allied biophysical approaches to the study of enamel mineralization. J R Micr Soc 83:135–141
7. Glas JE, Nylen MU (1965) A correlated electron microscopic and microradiographic study of human enamel. Arch Oral Biol 10:893–909
8. Frazier PD (1968) Adult human enamel: an electron microscopic study of crystallite size and morphology. J Ultrastruct Res 22:1–11
9. Towe KM, Hamilton GM (1968) Ultramicrotome induced deformation artifacts in densely calcified material. J Ultrastruct Res 22:274–281
10. Boyde A (1978) Cutting teeth in the SEM. Scanning 1: 157–165
11. Arends J, Jongebloed WL (1978) Crystallites dimensions of enamel. J Biol Buccale 6:161–171
12. Daculsi G, Kerebel B, Verbaere A (1978) Méthode de mesure des cristaux d'apatite de la dentine humaine en microscopie électronique à transmission de haute résolution. CR Acad Sciences Paris 286:1439–1442
13. Daculsi G, Kerebel B (1978) High resolution electron microscope study of human enamel crystallites: size, shape and growth. J Ultrastruct Res 65:163–172
14. Kerebel B, Daculsi G, Kerebel LM (1979) Ultrastructural studies of enamel crystallite. J Dent Res 58 (special issue B):844–850
15. Nylen MU, Eanes ED, Omnell KA (1963) Crystal growth in rat enamel. J Cell Biol 18:109–123
16. Selvig KA, Halse A (1972) Crystal growth in rat incisor enamel. The Anat Res 173:453–468
17. Warshawsky H, Nancy A (1982) Stereo electron microscopy of enamel crystallite. J Dent Res 61:1504–1514
18. Helmcke JG (1967) Ultrastructure of enamel. In: Miles AEW (ed) Structural and organization of teeth. Vol. II. Academic Press, New York
19. Leblond CP, Warshawsky H (1979) Dynamics of enamel formation in the rat incisor tooth. J Dent Res 58 (special issue B):950–975
20. Vogel SC, Weiss MP, Frank RM (1981) High resolution electron microscopic technique applied to the detection of distortions in apatite crystallites during amelogenesis. J Biol Buccale 9:183–191
21. Hammarlund-Essler E (1971) Trans Royal School of Dentistry, Stockholm and Umea. 4:15–25
22. Nylen MU (1979) Matrix-mineral relationships. A morphologist's viewpoint. J Dent Res 58 (special issue B):992–926
23. Meckel AH, Griebstein WJ, Neal RJ (1965) Ultrastructure of fully calcified human dental enamel. In: Stack MV and Fearnhead RW (eds) Tooth enamel, its composition, properties and fundamental structure. John Wright, Bristol, pp. 160–162
24. Menanteau J, Mitre D, Daculsi G (1984) Aqueous density fractionation of mineralizing tissues: an efficient method applied to the preparation of enamel fractions suitable for crystal and protein studies. Calcif Tiss Int, in press